Sea clutter model comparison for ship detection using single channel airborne raw SAR data

Sushil Kumar Joshi and Stefan V. Baumgartner, Microwaves and Radar Institute, German Aerospace Center (DLR), Oberpfaffenhofen, Germany

Abstract

Near real time processing of ship detection in a challenging ocean environment is imperative for maritime security and surveillance. Most of the sea clutter models developed for ship detection have been experimented over fully focussed SAR images. The goal of this paper is to evaluate the performance of clutter models on DLR's F-SAR acquired single-channel range-compressed data and range-Doppler image for on-board processing and high resolution ISAR image generation. K-distribution and tri-modal discrete (3MD) texture model were applied over the images and a good fit of these models were observed considering only the main beamclutter of the range-Doppler image. The work was further extended to detect ships at different false alarm rates.

1 Introduction

Ship detection using synthetic aperture radar (SAR) is an important component of maritime surveillance often limited due to the presence of sea clutter. Therefore, accurate modelling of sea surface clutter is a necessary procedure for the analysis of their impact on maritime target detection. The general idea of ship detection using sea clutter models is the computation of a detection threshold which is calculated based on constant false alarm rate [1]. The accuracy and robustness of the detection threshold at constant false alarm depends on how well the model fits to the distribution of sea clutter. Numerous statistical models have been previously used for calculating sea clutter statistics. Classical Rayleigh distribution works well for homogeneous regions of sea surface with coarser spatial resolution but fails in case of heterogeneous clutter with finer resolution [2]. There are other statistical distributions like log-normal, Gamma and Weibull distributions, which were found interesting for modelling sea clutter statistics. Among various distributions, the K-distribution is found to be a very promising tool for calculating amplitude statistics of sea clutter. It is popular because it is derived based on physical scattering process and reduces to Rayleigh distribution in case of homogeneous clutter [2], [3]. It is basically a compound model which is a comprehensive representation of Gaussian distributed homogeneous clutter and a gamma distributed texture random variable. Recently, a more sophisticated sea clutter model was developed known as tri-modal discrete (3MD) sea texture model, where the sea texture is statistically modelled in discrete form [4]. For spaceborne cases, this model performed better than K-distribution by taking into account the additive receiver noise. The model was also able to achieve a more practically relevant probability of false alarm detecting more target pixels. K-distribution, however, led to an overestimation of the detection threshold and thereby leading to missed targets.

Most of these models have been implemented on fully focussed airborne or spaceborne SAR images [5], which increase processing efforts and therefore are not ideal for real time applications. In order to achieve on-board processing in real time, there is a need to investigate the performance of these models in case of range-compressed images. Another necessary investigation is also on the range-Doppler images for inverse SAR (ISAR) imaging purposes which involves the generation of fine resolution images of non-cooperative moving targets [6].

The objective of this paper is to highlight the applicability of K-distribution and 3MD clutter model on range-compressed data and range-Doppler images. Initially, the sea clutter models are defined with their respective estimation parameters. These estimated parameters are then utilized to compute the detection thresholds based on a constant false alarm rate.

2 Sea clutter modelling

2.1 K-distribution pdf

K-distribution is a product model of Gaussian distributed homogeneous clutter and a gamma distributed texture variable whose probability density function (pdf) for a random amplitude x is defined as [4], [7].

$$f_T(x) = \frac{2\Gamma(v)^{-1}}{\Gamma(n)}\left(\frac{nv}{\sigma_c^2}\right)^{\frac{n+v}{2}} x^{\frac{n+v-2}{2}} K_{v-n}\left(2\sqrt{\frac{nv}{\sigma_c^2}}x\right). \quad (1)$$

T is the multilook statistics given as $T = \sum_{k=1}^{n}|Z_k|^2$, where Z_k is the amplitude data and n is the number of looks. Shape and scale parameters of the distribution are given by v and (v/σ_c^2), respectively. These parameters depend on sea conditions and radar parameters. $K(\cdot)$ is the modified Bessel function of the second kind. The range of v varies between $0.1 \leq v \leq \infty$; for $v = \infty$, the distribution reduces to Rayleigh distribution and $v < 1$ represents spiky clutter [7].

* The blue strip in between the image is due to the processing error which is however omitted for processing. In the final version of this paper, this error would be removed.

The probability of false alarm rate (PFA) for the multilook case is given as

$$P_{fa}(\eta) = 2\sum_{k=0}^{n-1} \frac{(vn)^{(v+k)/2}}{\Gamma(k+1)\Gamma(v)} \eta^{v+k/2} K_{v-k}(2\sqrt{vn\eta}). \quad (2)$$

The logarithmic form of eq. (2) shows that the P_{fa} is proportional to $-\sqrt{\eta}$.

2.2 Tri-modal discrete (3MD) texture model

This model is based on the idea of considering sea clutter as the function of finite and smaller number of distinct scatterer types. The pdf of discrete texture model is given as [4]

$$f_{\Delta}(\delta) = \sum_{i=1}^{I} c_i \partial(\delta - a_i) \quad (3)$$

Where $\sum_{i=1}^{I} c_i = 1,\ c_i > 0,\ \partial(\cdot)$ is the delta function and the unknown parameters a_i and c_i are the discrete texture intensity levels and their corresponding relative weightings, respectively. The continuous test pdf of 3MD model is written as

$$f_T(x, n, \odot) = \frac{n^n}{\Gamma(n)} x^{n-1} \sum_{i=1}^{I} c_i \frac{\exp\left(-\frac{nx}{\rho_c a_i^2 + \rho_n}\right)}{(\rho_c a_i^2 + \rho_n)^n}. \quad (4)$$

where $\odot$ = [c; a], ρ_c and ρ_n are the normalized clutter and noise variances whose sum is unity. The cdf is calculated as

$$F_T(x, n, \odot) = 1 - \sum_{i=1}^{I} c_i \frac{\Gamma\left(n, \frac{nx}{\rho_c a_i^2 + \rho_n}\right)}{\Gamma(n)}. \quad (5)$$

From (5), the PFA for a single-look data can be written as

$$P_{fa}(\eta, 1, \odot) = \sum_{i=1}^{I} c_i \exp\left(-\frac{\eta}{\rho_c a_i^2 + \rho_n}\right). \quad (6)$$

The logarithmic of PFA in this case is proportional to -η.

2.3 Parameters estimation

The estimation parameters in K-distribution are shape and scale parameters and in 3MD clutter model are the discrete texture intensity levels and their relative weightings. There are several methods that can be used for parameter estimation ranging from least square fitting, maximum likelihood (MLE) and method of moments (MoM) [8]. Methods like MLE and MoM are based on samples, ranging from hundreds to thousands. However, in this case the Levenberg-Marquardt algorithm (a non-linear least square approach) was adopted since the complete image was used after excluding the ship signal. It is an iterative technique to locate the minima of multivariate function that is expressed as a sum of the squares of non-linear real-valued functions.

3 Results and discussion

3.1 Time domain

Figure 1 shows the range-compressed data containing a ship. This single-channel X-band VV polarized image was acquired by DLR's F-SAR airborne system in 2016 in the North sea near Helgoland [6]. The ship covers the large area in the data.

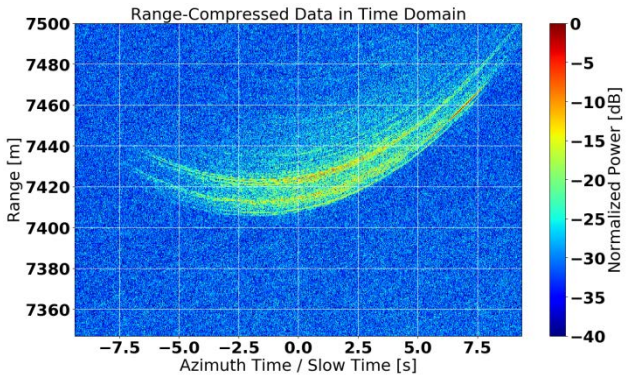

Figure 1: Range-compressed data with a ship.

K-distribution estimated parameter is applied over the ship free range-compressed image and is shown in Figure 2.

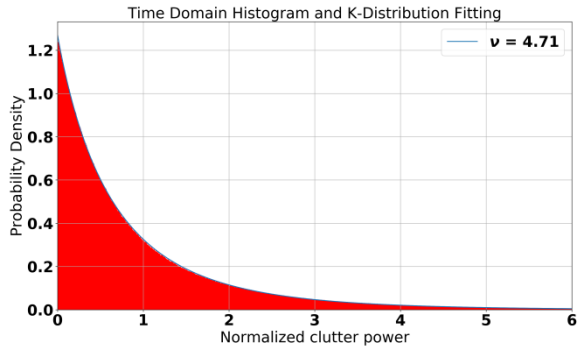

Figure 2: Histogram of range-compressed ocean clutter (red) and K-distribution fitting (blue).

As observed from Figure 2, the K-distribution fits the ocean clutter very well. Similarly, the 3MD clutter model fitting is shown in Figure 3. In this case for I = 3, which is mostly acceptable for various sea conditions is used [4].

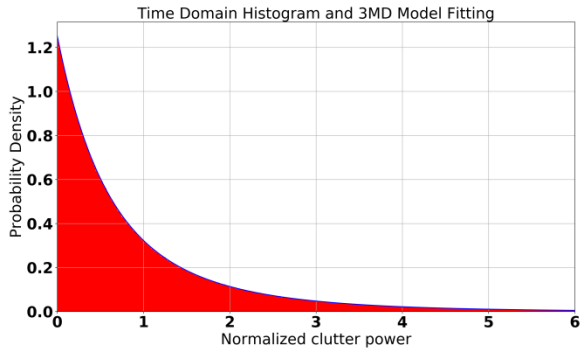

Figure 3: Histogram of range-compressed ocean clutter (red) and 3MD model fitting (blue).

The estimated parameters for the 3MD clutter model are $\odot = [0.383,\ 0.426,\ 0.190;\ 1.193,\ 0.910,\ 0.734]$. Figure 4 shows the curve plotted using logarithmic false alarm rate and the threshold for both K-distribution (red) and 3MD clutter model (blue) for ship free data. For smaller values of the threshold ($\eta \leq 6$), both curves show

a similar trend. However, for larger values of η, the red curve diverges whereas the blue curve is linear.

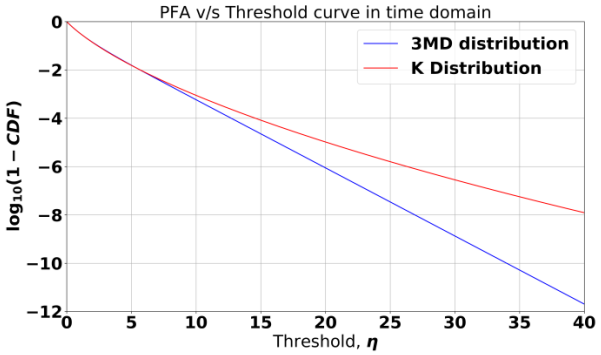

Figure 4: PFA v/s threshold for range-compressed data in time domain.

For a given PFA = 10^{-4}, the threshold estimates for both the distributions (K-pdf and 3MD) are 14.57 and 12.71, respectively, and for PFA $= 10^{-6}$ the corresponding threshold estimates are 26.29 and 19.80 respectively. Based on these thresholds, the ship pixels were detected and are shown in Figure 5 and Figure 6.

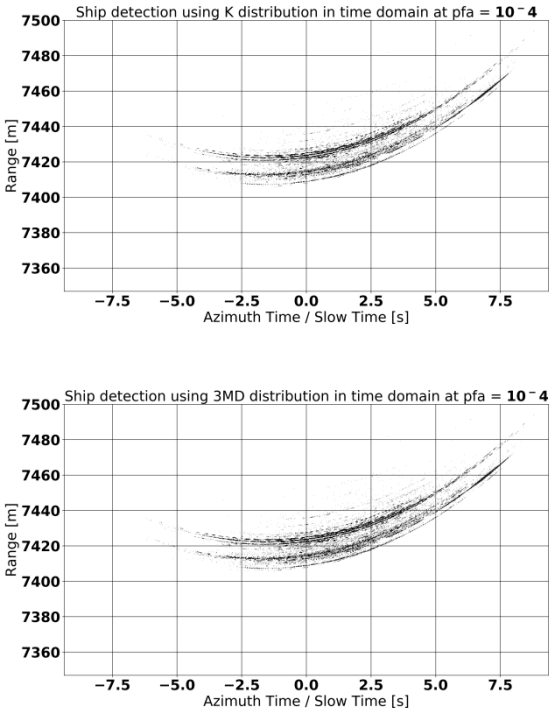

Figure 5: Ship detection for (a) K-pdf and (b) 3MD clutter model at PFA =$\mathbf{10^{-4}}$

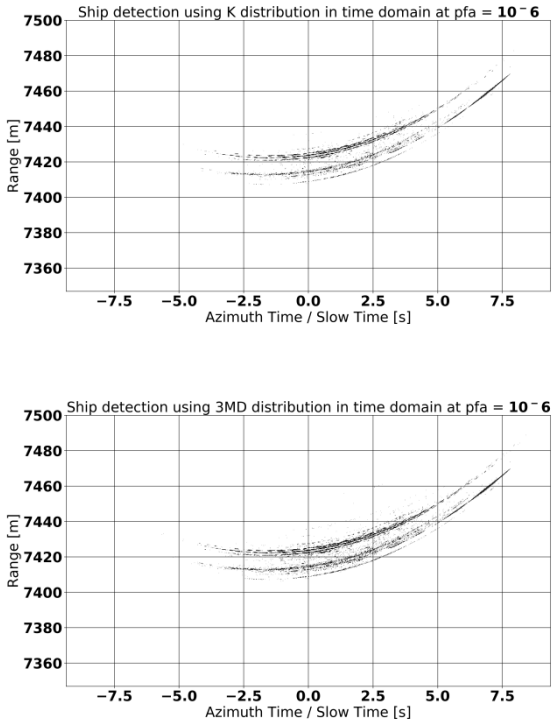

Figure 6: Ship detection results for (a) K-pdf and (b) 3MD clutter model at PFA =$\mathbf{10^{-6}}$.

Table 1 shows the number of ship pixel detections for each case. From the table it can inferred that for both PFAs, 3MD model gives more detections as compared to K-pdf due to the divergence of the curve shown in Figure 4.

PFA	K-PDF	3MD model
$\mathbf{10^{-4}}$	304320	362368
$\mathbf{10^{-6}}$	134011	201176

Table 1: Number of detections for both models using different PFAs

3.2 Range Doppler domain

This section discusses the implementation of K-PDF and 3MD model in range Doppler domain. A range-Doppler image is formed by computing the azimuth fast Fourier transform (FFT). One advantage of this domain is the shift of moving targets away from the main clutter beam. The target history can then be clearly distinguished from the clutter. The range-Doppler domain enables the detection of ships with low radar cross section, especially if they move with certain line-of-sight velocity.

The K-distribution and 3MD sea clutter models were applied only on the clutter part of the range-Doppler image. The clutter region is selected based on the 3dB clutter bandwidth which is 609.27 Hz with an estimated Doppler centroid of 271.63 Hz. Figure 7 shows the K-PDF curve fitting on the range-Doppler image.

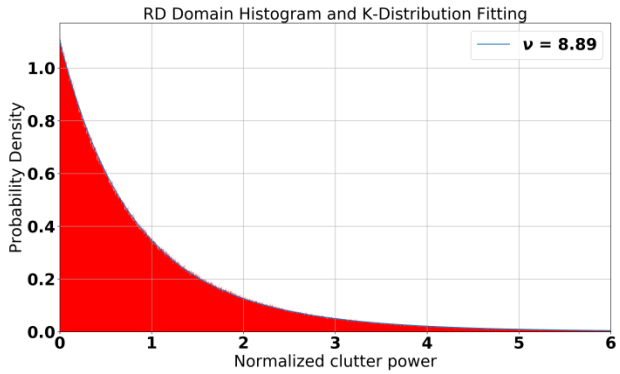

Figure 7: Range-Doppler domain histogram and K-distribution fitting for ocean clutter.

As observed from Figure 7, K-distribution fits well with the clutter region of the range-Doppler image. 3MD clutter model was also tested on this distribution and is shown in Figure 8.

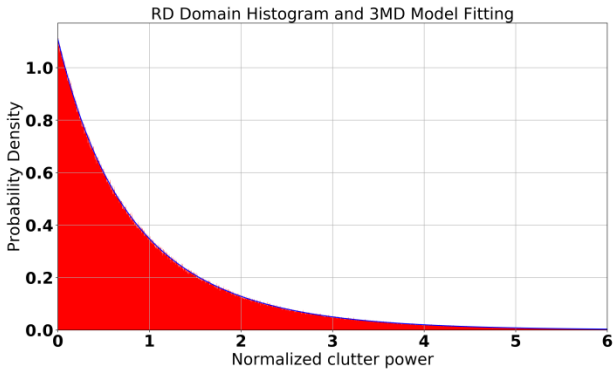

Figure 8: Range-Doppler domain histogram and 3MD model fitting for ocean clutter.

The 3MD clutter model is also found to have an almost perfect fit with the clutter only part of the range-Doppler image. The estimated parameters for this case are:
$\odot = [\,0.108, 0.792, 0.098; 1.183, 1.001, 0.755]$.
Figure 9 shows the PFA v/s threshold plot for both distributions in range-Doppler domain.

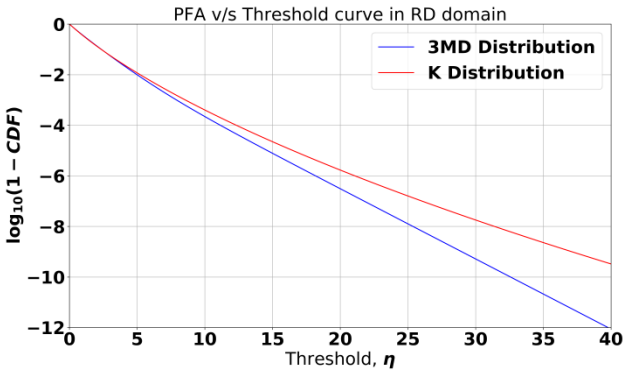

Figure 9: PFA v/s threshold in range-Doppler domain.

The curve shows the similar trend as in case of Figure 4. For higher thresholds $(\eta < 5)$ there is divergence for the red curve (K-PDF) whereas the blue curve fit well over the entire range.

3.2.1 Target detection in Range-Doppler

The advantage of carrying out target detection in range-Doppler domain is the increased signal-to-clutter plus noise ratio, especially for moving targets which are shifted to the exo-clutter region. Determining single threshold in case of time domain for both the pdfs is not sufficient in range-Doppler. If the threshold is decided based on only clutter then the target history is detected only around the clutter and if the threshold is computed based on the noise power then the complete clutter along with the target will be regarded as the target. Defining different models for different regions would increase the computation and processing efforts. Therefore, detection of moving targets in single-channel data in range-Doppler is a challenging task since the target history is present both in the noise and clutter region as shown in the Figure 10.

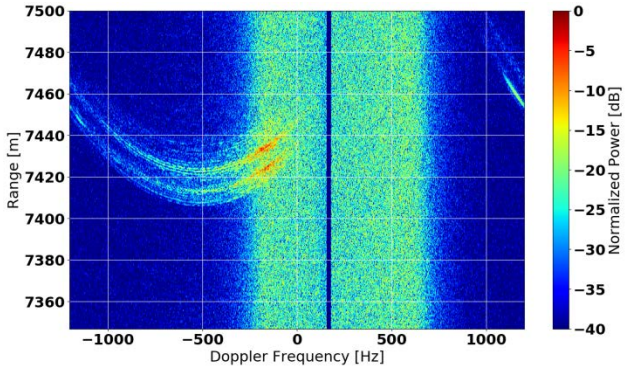

Figure 10: Range compressed data in Doppler domain. The history of the ship target is visible inside the main clutter beam. The blue strip at the center is a pre-processing artifact which will not be present in the final data product.

The main beam clutter in the figure is recognized by its high normalized power concentrated around the zero Doppler. From the figure, the presence of target in both the regions is clearly observed.
In order extract the full target history, clutter whitening is a necessary step and it is achieved through the normalization of power spectral density (PSD) of the data containing the target and the average spectra along range of the target free data [9]. This results in the clutter whitening leaving the target history undisturbed. If $S_r(f)$ and $N_r(f)$ are the PSDs of the target and target free data and $A_r(f)$is the average spectra for ship free data, and all are defined over the Doppler bins f and total range R then the normalization is obtained as $S_r(f)/A_r(f)$, where

$$A_r(f) = \frac{1}{R}\sum_{r=0}^{R-1} N_r(f) \qquad (7)$$

The image of the ship data after normalization is shown in Figure 11.

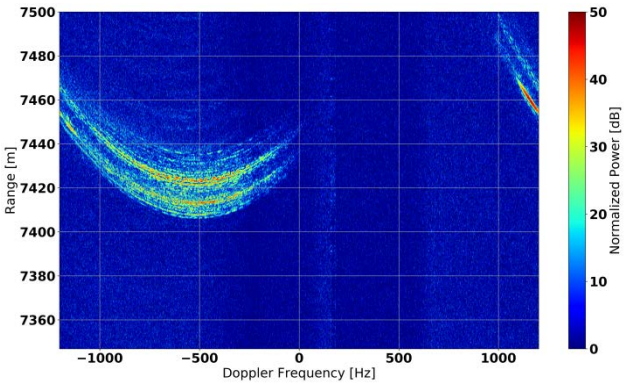

Figure 11: Post Doppler whitening result.

From the figure, the true history of the target is clearly observed and the clutter is suppressed to a great extent. Clutter models can then be applied onto the clutter suppressed data to obtain the required threshold for target detection.

4 Conclusion

This paper demonstrated the applicability of the K-distribution and 3MD clutter model on range-compressed data in time as well as in range-Doppler domain. For both cases, these models fit very well with the ocean clutter distribution. The 3MD clutter model gives more detections of ship pixels for different PFAs due to lower detection thresholds which can possibly include more false detections. However, with a high detection threshold weak reflections from the target might be rejected. In such cases, where the signals are weak due to low radar cross section, it is important to improve the signal to noise ratio by considering coherent processing intervals. Since the detection threshold so far is based on the clutter region, for detection in range-Doppler domain, normalization of the clutter was an important step to proceed further with the target detection. This resulted in the retrieval of complete profile of the target. However, the present solution rely on the the target free homogeneous sea clutter environment which is generally not the case keeping in mind the near real time processing problems. A robust and efficient method is still under investigation which would perform pre-detection of moving targets before post-Doppler whitening and true target profile estimation.

5 Literature

[1] A. Farina and F. A. Studer, “A review of CFAR detection techniques in radar systems,” *Microw. J.*, vol. 29, no. 115, pp. 179–185, 1986.

[2] E. Jakeman, “On the statistics of K-distributed noise,” *J. Phys. A. Math. Gen.*, vol. 13, pp. 31–48, 1980.

[3] K. D. Ward, “Compound representation of high resolution sea clutter,” *Electron. Lett.*, vol. 17, no. 16, pp. 561–563, 1981.

[4] C. H. Gierull, I. C. Sikaneta, R. Defence, and D. C. Drdc, “Improved SAR Vessel Detection Based on Discrete Texture,” *Proc. EUSAR 2016 11th Eur. Conf. Synth. Aperture Radar*, pp. 523–526, 2016.

[5] A. Marino, M. Sanjuan-Ferrer, I. Hajnsek, and K. Ouchi, “Ship Detection with Spectral Analysis of Synthetic Aperture Radar: A Comparison of New and Well-Known Algorithms,” *Remote Sens.*, vol. 7, no. 5, pp. 5416–5439, 2015.

[6] S. V Baumgartner, “Linear and Circular ISAR Imaging of Ships Using DLR ’ s Airborne Sensor F-SAR,” in *IET Radar*, 2017.

[7] K. D. Ward, R. J. A. Tough, and S. Watts, “Sea clutter: Scattering, the K distribution and radar performance,” *Waves in Random and Complex Media*, vol. 17, no. 2, pp. 233–234, 2007.

[8] I. R. Joughin, D. B. Percival, and D. P. Winebrenner, “Maximum likelihood estimation of K distribution parameters for SAR data,” *Geosci. Remote Sensing, IEEE Trans.*, vol. 31, no. 5, pp. 989–999, 1993.

[9] L. Rosenberg and S. Watts, “Model based coherent detection in medium grazing angle sea-clutter,” in *2016 IEEE Radar Conference, RadarConf 2016*, 2016.